Electro-Optical Generation and Distribution of Ultrawideband Signals Based on the Gain Switching Technique

Haymen Shams, Aleksandra Kaszubowska-Anandarajah, Philip Perry, P. Anandarajah, and Liam P. Barry

***Abstract*—We demonstrate and compare the generation and distribution of pulse position modulation (PPM) ultrawideband (UWB) signals, based on two different techniques using a gain-switched laser (GSL). One uses a GSL followed by two external modulators, while the second technique employs two laser diodes gain switched (GS) using a combined signal from a pattern generator and an RF signal generator. Bit-error-rate (BER) measurements and eye diagrams for UWB signals have been measured experimentally by using the different GS transmitter configurations and various fiber transmission distances. The simulation of both systems also has been carried out to verify our obtained results, which show the suitability of employing gain switching in a UWB over fiber (UWBoF) system to develop a reliable, simple, and low-cost technique for distributing the impulse-radio UWB (IR-UWB) pulses to the receiver destination.**

***Index Terms*—Fiber optics communications; Radio frequency photonics**.

I. Introduction

Demands in wireless data transfer required from the end users have been increasing dramatically. Nowadays, users need high-speed wireless access networks to share photos, music, videos, and even high-definition video streams. Ultrawideband (UWB) technology is an excellent and a reliable solution for future wideband wireless personal access networks (WPANs) and high-bit-rate communication [1,2]. This is due to its benefits of lower power consumption, low cost, high data capacity, and immunity to multipath fading. UWB is a short-range (~10 m) wireless communication due to its power limitation from the Federal Communications Commission (FCC) regulation [3]. The FCC allocated in 2002 the unlicensed frequency band between 3.1 to 10.6 GHz for indoor UWB wireless communication systems with a power spectral density (PSD) lower than −41.3 dBm/MHz. One of the main modulation schemes in UWB is impulse radio (IR-UWB), which uses a carrier-free transmission with very narrow pulses [4]. IR-UWB is an attractive method due to its carrier-free modulation, lack of complicated frequency mixers, lack of intermediate frequency, and by consequence low power consumption and low cost. However, to increase its coverage area, UWB signals can be easily integrated with optical links that provide low cost, low loss, and extremely large bandwidth [5,6]. This technique is known as UWB over fiber (UWBoF) and can be used for distributing UWB signals from the central station to different remote base transceiver stations. Hence, UWBoF can be used to extend the coverage of UWB to hundreds of meters using optical fiber inside a building or a medium-range network in the home or office.

Several schemes for UWBoF have been proposed recently that depend on the optical generation of the impulse radio [7–11]. The generation of Gaussian monocycles and doublets as an impulse signal have been reported in many research schemes for UWB systems. It has been demonstrated that these pulses have a wider 3 dB bandwidth, and better performance in terms of bit error rate (BER) and multipath immunity in comparison with other signals [12]. These pulses can be created by using bandpass filtering of Gaussian pulses to take the first- and second-order derivatives of the signal. UWB monocycle pulses have been generated by using a gain-switched laser (GSL) and microwave bandpass filter after the photodetector in [7], whereas other techniques have shown the optical gen-

Manuscript received September 18, 2009; revised January 13, 2010; accepted January 13, 2010; published February 18, 2010 (Doc. ID 116917).

The authors are with the Research Institute for Networks and Communication Engineering (RINCE), Department of Electronic Engineering, Dublin City University, Dublin 9, Ireland (e-mail: haymen.shams@eeng.dcu.ie).

Digital Object Identifier 10.1364/JOCN.2.000122

1943-0620/10/030122-9/$15.00

eration of UWB signals based on optical phase modulators with dispersive devices or an optical frequency discriminator, a photonic microwave delay-line filter, or optical spectral shaping [8]. The pulse modulation scheme is also an important aspect of UWB distribution systems. Several modulation schemes have been employed in order to satisfy the application and the design parameters such as pulse amplitude modulation (PAM), on–off keying (OOK), pulse position modulation (PPM), and binary phase-shift keying (BPSK) [13]. The implementation of an experimental UWBoF system for distributing IR-UWB signals based on OOK pulses has been carried out in [9,10] and the optical BPSK modulation scheme to generate biphase Gaussian monocycle pulses has been carried out in [11]. In this paper, we demonstrate two different approaches for the generation and distribution of electro-optic IR-UWB signals based on a GSL and PPM modulation scheme at a bit rate of 1.625 Gbps. The first technique is based on using one GSL and two Mach–Zehnder modulators (MZMs) for external data modulation [14], whereas the second approach is based on a directly modulated (DM) GSL. The second approach uses a simpler direct modulation scheme for conversion of the electrical non-return-to-zero (NRZ) data signal to optical return-to-zero (RZ) data [15,16]. To explore the trade-off between cost, performance, and reach, the performance of the two system setups has been evaluated using experimental implementations and simulations over different fiber links by using three different configurations of a GSL diode transmitter.

The structure of this paper is organized as follows. Section II gives an overview of our optical distribution system. Section III outlines the experimental and simulation results using the first transmitter setup for the electro-optic generation of IR-UWB based on a GSL and two external modulators. Section IV then goes on to present the experimental and simulation results of the second approach using two directly modulated GSLs, and finally Section V presents a summary and conclusion.

II. System Overview

The major building block of our system is the optical distribution system, shown in Fig. 1. It consists of a central node or an optical distribution center (ODC) that generates a PPM optical signal using a GSL and a pulse pattern generator (PPG) at 1.625 Gbps. These optical signals are then distributed through fiber links to a number of remote antenna units (RAUs). In the RAU, the signals are photodetected, shaped to UWB signals using an electrical bandpass filter (BPF), and radiated through air to the radio terminal (RT). At the user end (the RT), the UWB signals are amplified and

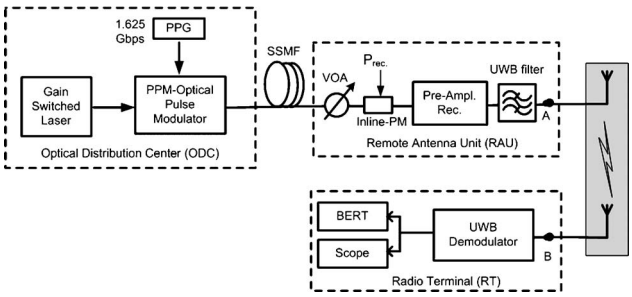

Fig. 1. Block diagram of our proposed optical distribution system.

demodulated. The system performance has been verified by using a bit-error-rate tester (BERT) and a high-speed digital sampling scope. This system allows for the transmission of broadband data over hundreds of meters, with possible application areas of the proposed system involving the distribution of high-quality video stream content from DVDs and personal video recorders to high-definition television (HDTV) displays. In the next two sections, we will present two different setups for generating PPM optical signals. The first one is achieved by using a pair of external modulators driven by a pattern generator, while the second one is achieved by combining the signal from a pattern generator and an RF signal generator and using the composite signal to gain switch two lasers.

III. Generation of IR-UWB by Using Two External Modulators

A. Experimental Setup

The schematic diagram of the first proposed system is shown in Fig. 2. In the ODC section, the optical pulses are generated using the technique of gain switching. Three different laser configurations, operating at 1550 nm, were used for the gain switching: a Fabry–Perot laser diode (FP-LD), a distributed-feedback laser diode (DFB-LD), and an externally injected DFB-LD (EI DFB-LD). The FP-LD used was a commercially available InGaAsP device with a threshold current of 9 mA. The DFB-LD was a commercial NEL laser within a 14 pin butterfly package. The EI DFB-LD is composed of a modulated DFB laser and a continuous-wave (CW) DFB-LD in a master–slave configuration [17]. The optical spectra for the three GSLs are shown as insets (i), (ii), and (iii) in Fig. 2, respectively.

The gain switching of the lasers is achieved by applying a bias below threshold in conjunction with an amplified sinewave at a repetition rate of 1.625 GHz. The gain-switched (GS) pulses, which are of the order of 20 ps width, are shown in inset (iv) in Fig. 2. These optical pulses are divided into two equal paths by using a 50:50 coupler. A pseudorandom bit sequence

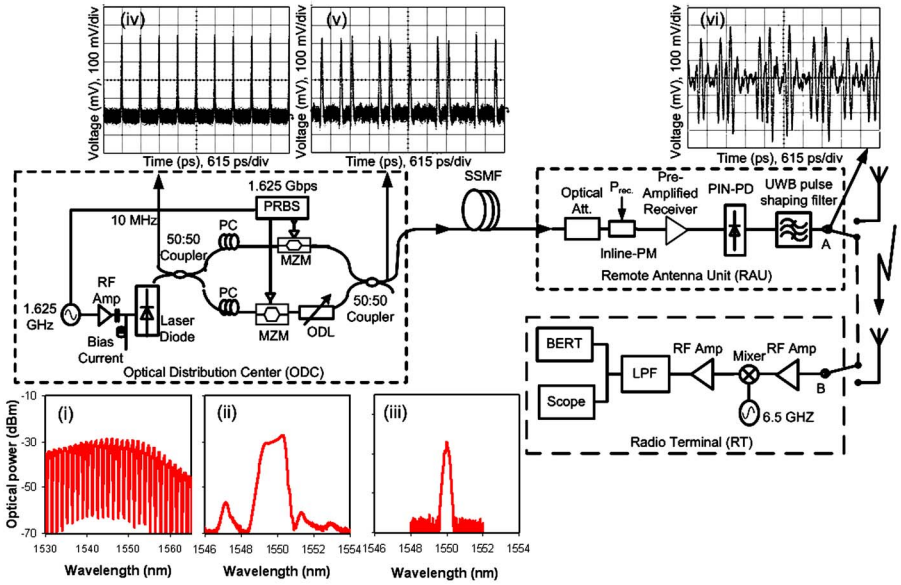

Fig. 2. (Color online) Experimental setup for generating PPM pulses by using two external modulators: (i), (ii), and (iii) optical spectra for gain-switched FP, DFB, and EI DFB, respectively; (iv) gain switched pulses; (v) PPM pulses; (vi) doublet Gaussian pulses.

(PRBS) of length 2^7-1 at a bit rate of 1.625 Gbps from a PPG is applied to the MZMs. The data output (D) of the PPG is used to drive the upper MZM (passing pulses for all logical 1's), while the complementary output ($\bar{D}$) of the PPG is used to drive the lower MZM (passing pulses for all logical 0's). The output pulses from the lower MZM are then delayed using an optical delay line (ODL) before being combined with the output of the upper MZM. This composite waveform represents a PPM signal as shown in inset (v) of Fig. 2 for the DFB-LD case for a sequence of 0010110100, which is then transmitted along different lengths of standard single-mode fiber (SSMF) to the RAU. At the RAU, an optically preamplified receiver consisting of an erbium-doped fiber amplifier (EDFA), an optical bandpass filter (OBPF), and a p–i–n photodetector (PIN-PD) is used to convert the optical pulses into electrical pulses.

These electrical pulses are amplified and shaped to a UWB signal by using an electrical UWB filter (bandpass 3.1–10.6 GHz), which acts as a differentiator and converts these Gaussian pulses into doublet Gaussian pulses. These pulses are shown as inset (vi) in Fig. 2 for the DFB-LD case and are broadly similar for the other lasers tested. The electrical RF spectrum at point A is adjusted to meet the stringent FCC's mask and is shown in Fig. 3, and the dotted line represents the S21 of the UWB filter. Here the spectrum shaping is achieved by the filter and the amplitude is adjusted to meet the mask by setting the optical received power using a variable optical attenuator. The output of the filter is then connected directly to point B in the RT, since we focus only on the UWB signal degradation over the fiber transmission link. At the RT, the signal is amplified and mixed with a 6.5 GHz signal (the fourth harmonic of 1.625 GHz) from the local oscillator (LO) to downconvert the UWB signal to baseband. The output from the mixer is then amplified and filtered with a low-pass filter (LPF) to remove the unwanted frequency components yielding a demodulated data signal. BER measurements are then performed for a back-to-back (BTB) case as well as for different fiber lengths placed between the ODC and RAU. A variable optical attenuator (VOA) is used with an inline powermeter to enable the monitoring of the optical received power (P_{rec}) before the preamplified receiver during the measurements of the BER. Eye diagrams are also recorded at the output of the RT by using a high-speed digital sampling oscilloscope.

It should also be noted that the simple demodulator used in this experiment requires at least three main

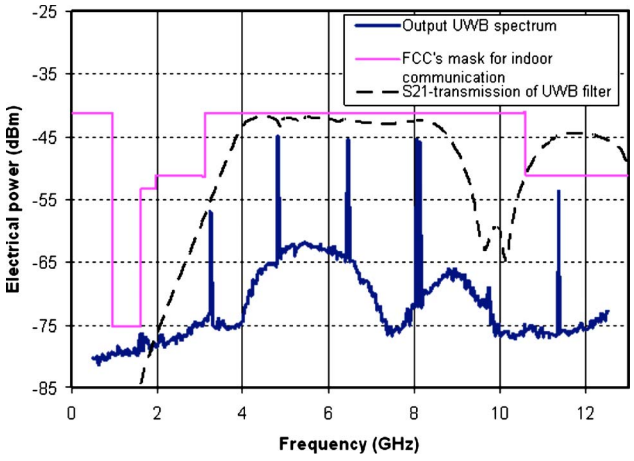

Fig. 3. (Color online) Electrical spectrum for the generated PPM electrical UWB pulses.

tones within the electrical spectrum and is therefore constrained to bit rates of less than 3–4 Gbps. For the particular UWB bandpass filter used in this experiment, the maximum bit rate is approximately 1.7 Gbps. It is expected that the use of a different electrical filter and advanced signal processing at the demodulator would increase this maximum rate.

B. Results and Discussions

In Fig. 4, the BER is plotted versus the received optical power at the RAU for the three different optical transmitters. The eye diagrams corresponding to each of the transmitter configurations are shown as insets in each of the figures. Figure 4(a) shows that the GS FP-LD can be used to achieve error-free performance (BER $< 10^{-9}$) while transmitting over fiber lengths up to 450 m. The degraded performance over 650 m is mainly due to mode partition noise (MPN). Dispersion in the fiber causes the fluctuations of the energy between the longitudinal modes of the FP-LD to be translated into intensity fluctuations on the transmitted optical signal, thus reducing its signal-to-noise ratio [18]. Another contributory factor to the performance degradation is the amplified spontaneous emission (ASE) from the EDFA (because no ASE removal filter is used). Optical filtering cannot be employed with this multimode transmitter scenario because it would worsen the effect of MPN [18]. In the case of the DFB laser [Fig. 4(b)], near-error-free transmission, while transmitting over 1 km of SSMF, can be achieved. In this case the system transmission reach is limited by noise resulting from the degradation in the side mode suppression ratio (SMSR) of the laser (~10 dB for gain-switched DFB), which causes MPN problems as outlined above for the FP laser, as well as a relatively large temporal jitter (5 ps) in the generated optical pulses. By employing external light injection [19], the performance of the DFB-LD can be greatly improved as shown in Fig. 4(c). This improvement is achieved as a result of the enhancement of the pulse SMSR (> 30 dB), which eliminates MPN, and a reduction of the temporal jitter (< 1 ps). Hence, with this transmitter configuration, error-free transmission over 37 km of SSMF has been achieved.

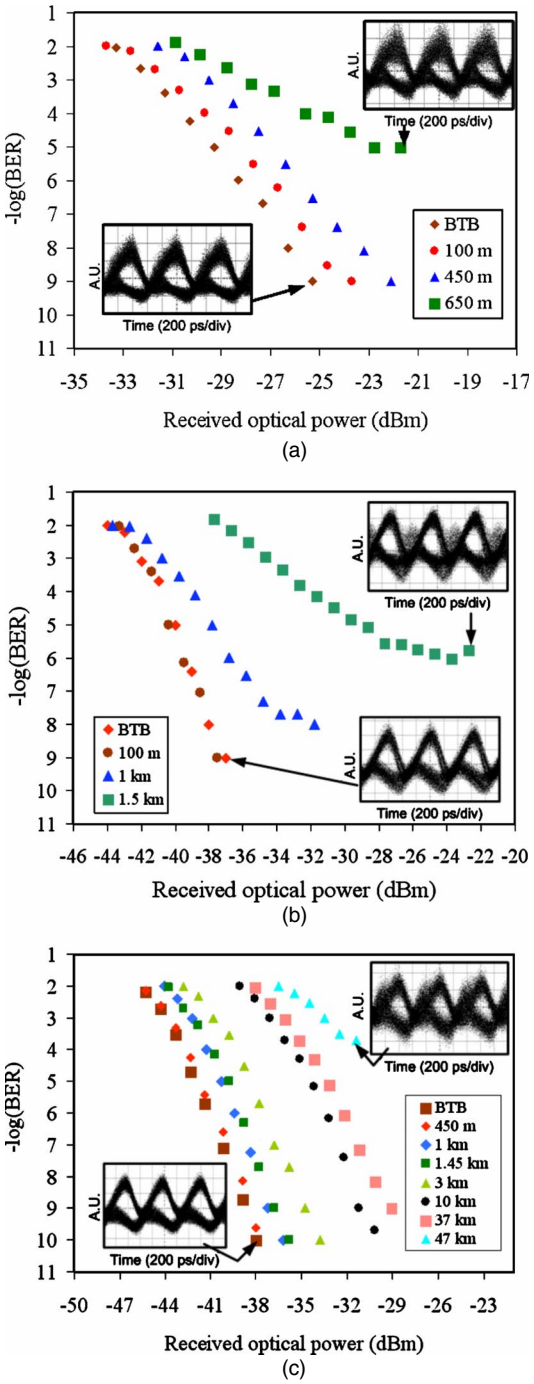

Fig. 4. (Color online) Measured BER versus received optical power for different SSMF links and the eye diagram for the lowest BER using three different transmitter configurations: (a) FP-LD, (b) DFB-LD, and (c) EI DFB-LD.

C. Simulation Results

Simulations have also been carried out by using the VPItransmissionMaker simulation platform to model the proposed setup and verify our experimental results. The key parameters of the devices have been chosen to meet the real experimental parameters. The GSL was simulated by using a transmission line model (TLM) of a semiconductor laser module at a wavelength of 1550 nm, and the output pulses were optimized by adjusting the bias and amplitude of the RF drive. In the case of the EI DFB-LD, a CW module laser was used to realize the external injection. The wavelength and power of the CW module laser were optimized to obtain pulses exhibiting low jitter and a narrow optical spectrum. We also used a SSMF with a group velocity dispersion (GVD) of 16 ps/nm/km and a loss of 0.2 dB/km. The optical receiver has a ther-

mal noise with 10^{-11} A/(Hz)$^{1/2}$ and a responsivity of 1 A/W. In the downconversion at RT, the local oscillator phase was adjusted to give the lowest BER and an open eye diagram for each transmission distance. The simulation results for the BER versus the received optical power for the three configurations are shown together in Fig. 5, and the simulated eye diagrams are also shown in Fig. 6. These results show the system performance for each of the three transmitter configurations for BTB and maximum transmission reach scenarios. For the FP-LD, the simulation illustrates that ASE noise causes the FP-LD to portray the worst receiver sensitivity in the BTB case, and an error floor could be seen at a BER of 10^{-11}. The maximum reach (650 m) is caused primarily by the multimode spectrum, which, when transmitted, results in MPN as discussed in Subsection III.B. The simulated eye diagram for BTB and after transmission over 650 m are shown in Figs. 6(a) and 6(b). In the case of the DFB-LD an improvement in the BTB receiver sensitivity is achieved mainly due to the removal of ASE with the use of an OBPF. However, the maximum transmission reach can only be doubled due to the degraded SMSR of the GS-DFB, which results in MPN. Figures 6(c) and 6(d) show the simulated eye diagram for the BTB and after transmission over 1500 m. The EI DFB-LD exhibits the best BTB receiver sensitivity as a result of the reduced pulse-to-pulse jitter. Moreover, it also achieves the maximum reach, which can be attributed to the enhanced SMSR, reduced jitter, and reduced chirp. This can also be seen in the simulated eye diagram for the BTB case in Fig. 6(e). From Fig. 6(f), after transmission over a fiber link of 47 km, the eye diagram is degraded due to the combined effect from the fiber's attenuation and dispersion; however, it is clear that we are able to achieve a significant increase in performance and reach with the EI-DFB. The experimental and simulated results are also summarized in Table I to show the performance for the three transmitter configurations. The table demonstrates that there are small differences between the simulated and experimental measurements in the receiver sensitivities for BTB and the power penalty needed for maximum reach at BER$<10^{-9}$.

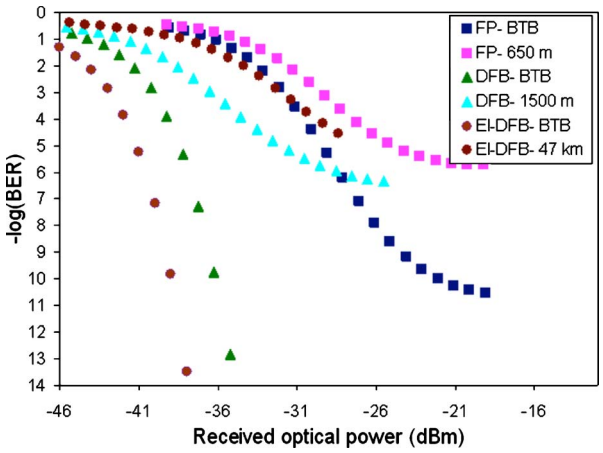

Fig. 5. (Color online) Simulated BER versus received optical power for the three different GSLs.

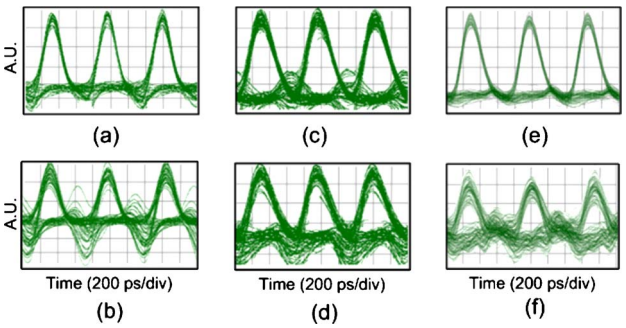

Fig. 6. (Color online) Simulated eye diagrams for FP lasers at (a) BTB and (b) 650 m, DFB lasers at (c) BTB and (d) 1500 m, and EI-DFB lasers at (e) BTB and (f) 47 km.

IV. Generation of IR-UWB by Using Direct Modulation for the Laser

A. Experimental Setup

The schematic diagram for the second approach for the UWBoF distribution system is shown in Fig. 7. The ODC uses the simpler direct modulation of a GSL for data transmission at a rate of 1.625 Gbps. The ODC setup consists of two DFB-LDs biased below the threshold current value via a bias tee. These two DFB-LDs are modulated using a combination of a 1.625 GHz sinusoidal signal generator and a synchronous 1.625 Gbps pattern generator (2^7-1 PRBS). The output from the signal generator is amplified and then divided into two equal paths before it is combined with the NRZ data pattern for both data and inverted data. The resultant output waveforms are applied to both DFB-LDs to generate Gaussian pulses through the GS process only when the data signal applied to the laser is a bit 1. The output pulses are adapted using the inspection of the eye diagrams to the best extinction ratio and minimum pattern-dependent effect by adjusting the bias level and the amplitude of the electrical data. DFB-LD 1 generates a GS Gaussian pulse for each logical bit 1, while DFB-LD 2 generates a GS Gaussian pulse for each logical bit 0.

The output from both lasers are then delayed relative to one another by using the optical delay line (ODL) before the data and inverted data pulses are combined using a 50:50 coupler and then transmitted directly as a PPM signal over different lengths of SSMF. After fiber transmission, the signal is received by the same RAU and RT (shown in Fig. 2), which amplifies the received PPM signal and transforms it into electrical UWB pulses. Then, the UWB signal is transmitted directly to the RT at point B to be demodulated

TABLE I
RESULTS SUMMARY FOR IR-UWB GENERATION BY USING TWO EXTERNAL MODULATORS

Transmitter Configuration		BTB Threshold at 10^{-9} (dBm)	Power Penalty for Max. Reach at 10^{-9} (dB)	Maximum Reach	Error Floor Value	Longer Transmission for Error Floor
FP-LD	meas.	−25.3	3.2	450 m	10^{-5}	650 m
	simul.	−25.1	3.5	450 m	10^{-6}	650 m
DFB-LD	meas.	−37.5	5.7	1 km	10^{-6}	1.5 km
	simul.	−38.2	4.7	1 km	10^{-6}	1.5 km
EI DFB-LD	meas.	−38.9	9.9	37 km	10^{-4}	47 km
	simul.	−39.9	10.2	37 km	10^{-4}	47 km

and amplified. BER measurements and eye diagrams are recorded for the received signal over different fiber lengths.

B. Results and Discussion

The system performance is measured using two different configurations of our DM GS laser transmitters. In the first configuration we simply used two GS DFB laser diodes (DFB-LD) operating at the same wavelength and their optical spectrum is shown in Fig. 7 inset (i). While in the second configuration, we externally injected light from a third laser in a CW mode into the two GS DFB lasers to give an externally injected GS DFB (EI DFB-LD) laser and have the optical spectrum shown as in Fig. 7 inset (ii). Due to the limited practical components, the DFB-LDs and EI DFB-LDs were chosen with different operating wavelengths. The oscilloscope traces in Fig. 8 show the NRZ data, the laser drive signal consisting of the data combined with the RF sinusoid, and the resulting optical pulses. It is interesting to note that the data needs only to create a small offset to generate narrow pulses with a good extinction ratio. The two optical outputs, which have pulse durations of around 20 ps, are combined together after delaying the lower branch by 285 ps relative to the beginning of a bit period. The BER measurements for the different fiber spans versus the received optical power at the RAU (P_{rec}) are shown in Fig. 9. Figure 9(a) shows an error floor at 10^{-8} due to significant levels of amplitude noise and temporal jitter on the GS pulses. This limits the performance but is acceptable for a radio-based system that includes a high level of forward error correction. The results also show a penalty of 0.7 dB between BTB and 1 km transmission at a BER of 10^{-8}.

However, the system reaches an error floor at around 10^{-5} on transmission over 10 km fiber due to the large frequency chirp on the GSL that broadens the spectrum to approximately 1 nm. The fiber dispersion results in the chirped pulses being significantly broadened such that the 1 and 0 data pulses overlap causing intersymbol interference (ISI). The eye diagrams are also shown in Fig. 9(a) as insets for the lowest bit error rate at 1 km and after transmission over 10 km. When we employ the EI GS-DFB laser diodes we greatly improve the performance of the system transmission. The result shown in Fig. 9(b) reveals that the transmission length is extended up to 10 km with error-free (BER=10^{-9}) performance. It should be noted that the receiver sensitivity in the BTB case has

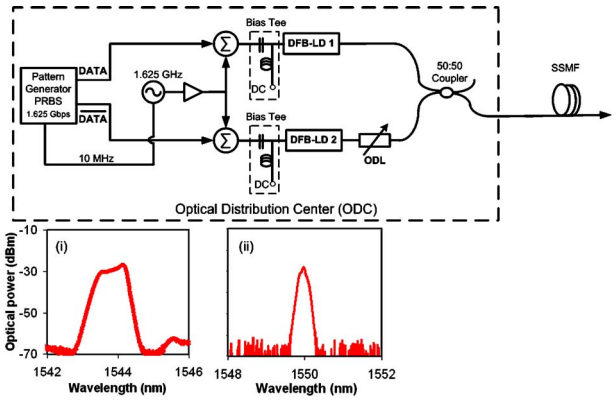

Fig. 7. (Color online) Schematic diagram for generating PPM by using two directly modulated GSLs: (i) and (ii) optical spectra for directly modulated gain-switched DFB and EI DFB.

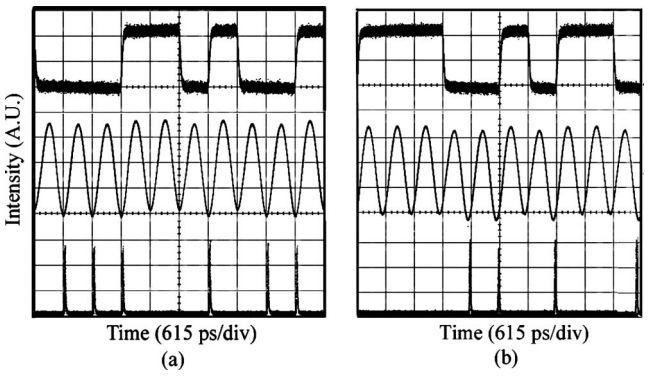

Fig. 8. Data, combined data, and an RF sinusoid and output pulses from lasers for (a) data and (b) inverted data at 1.625 Gbps.

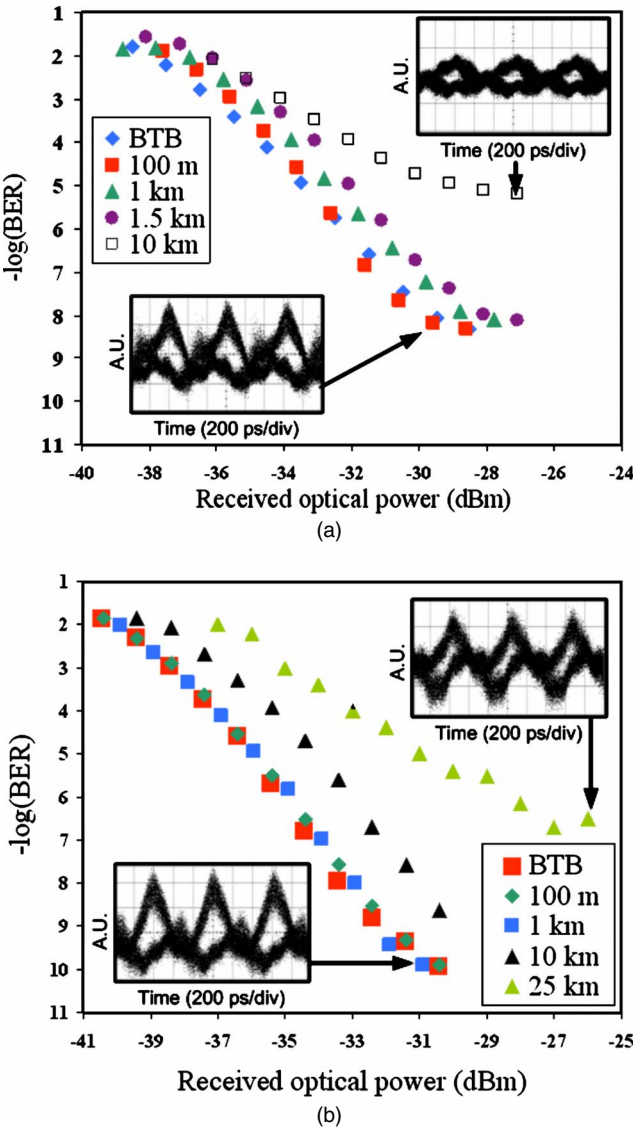

Fig. 9. (Color online) Measured BER versus received optical power for different SSMF spans and the eye diagrams for two different transmitter configurations: (a) two GS-DFBs, (b) two EI GS-DFBs.

been improved by 3 dB compared with the noninjected case due to the reduction of timing jitter (from ~4 to <1 ps) and the enhancement in SMSR (from ~10 to >30 dB) of the GS-DFB lasers, which reduces MPN caused by optical filtering in the experiment [18]. In the EI GS-DFB case, the system displays an error floor around 10^{-7} for a distance of 25 km. As for the noninjected case, this error floor is a result of ISI between the 1 and 0 data pulses. The significantly extended reach in the EI GS-DFB case is due to the chirp reduction caused by the external injection (spectral width reduced from ~1 to ~0.3 nm) [20].

C. Simulation Results

The simulated model for the generation and distribution of hybrid UWB signal using directly modulated

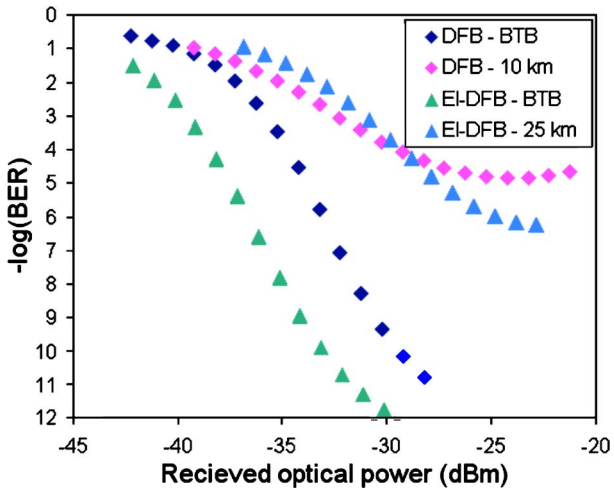

Fig. 10. (Color online) Simulated BER versus received optical power for two transmitter configurations of the two directly modulated GSLs.

lasers has been carried out for the noninjected and injected case. We used here two TLM semiconductor laser modules with the same biased and RF drive power combined with both data and inverted data to achieve the DM GS DFB-LD. The BER versus received optical power is shown in Fig. 10 and the simulated eye diagrams are also shown in Fig. 11 for the direct modulated GS-DFB and EI GS-DFB. Figures 11(a) and 11(b) illustrate the simulated eye diagrams for DFB-LD and demonstrate the timing jitter and MPN effect in the downconverted pulse between BTB and 10 km transmission over fiber. These detrimental effects are eliminated in the injected case as shown by the eye diagrams in Figs. 11(c) and 11(d) for BTB and transmission over 25 km. However, this transmitter configuration shows a maximum reach only to 25 km in EI GS-DFB, which is significantly different from the first configuration, which could achieve 37 km error free. This is mainly due to the degradation in the extinction ratio in the direct modulation case compared with that in the external modulators.

The important results from the directly modulated GS laser are summarized in Table II. The table clearly

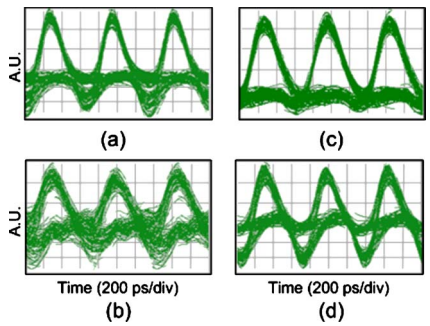

Fig. 11. (Color online) Simulated eye diagrams for DM DFB-LD at (a) BTB and (b) 10 km and DM EI DFB-LD at (c) BTB and (d) 25 km.

TABLE II
RESULTS SUMMARY FOR IR-UWB GENERATION BY USING TWO DIRECTLY MODULATED GSLS

Transmitter Configuration		BTB Threshold at 10^{-9} (dBm)	Power Penalty for Max. Reach at 10^{-9} (dB)	Maximum Reach	Error Floor Value	Longer Transmission for Error Floor
DM DFB-LD	meas.	−29.5	2.4	1.5 km	10^{-6}	10 km
	simul.	−31.2	3.1	1.5 km	10^{-5}	10 km
DM EI DFB-LD	meas.	−33.4	2	10 km	10^{-7}	25 km
	simul.	−34.1	2.3	10 km	10^{-7}	25 km

shows that there is a close match between experimental and simulation results. The simulated and experimental BER shows a 1 dB difference in BTB. The power penalty is about 2 dB for the maximum reach for both cases at 10^{-9}, while the error floor is nearly the same for the longest transmission distance for DFB and EI DFB at 10 and 25 km, respectively.

The advantage of the direct modulation scheme over the previous setup is its simplicity as it does not require external modulators, and hence there is no additional insertion loss, and a reduction in cost, which is vital for the development of a low-cost solution for distribution of UWB signals. In Table III, the comparison between the two distribution setups is presented in terms of the limiting factors that affect the system distribution and the required costs. In systems that need the distribution for a small residential network or office building, the FP-LD or DM DFB-LD can be the best choice for a low-cost and easily integrated system. However, for a large distribution system, the EI DFB-LD scheme with two external modulators allows a more reliable and stable system for many end users with maximum reach.

V. CONCLUSIONS

UWB over fiber is an attractive and cost-effective solution for increasing the reach of UWB systems. In this work, we have successfully demonstrated the generation and distribution of 1.625 Gbps UWB signals modulated in PPM format by using two optical distribution setups. Both setups have been studied over different fiber links using different GS laser configurations. The first approach uses one GS laser and two external modulators. The results show that error-free transmission can be achieved for the GS FP, DFB, and EI DFB laser transmitters over 450 m, 1 km, and 37 km, respectively.

We have also demonstrated an alternative approach for the generation and distribution of UWB signals based on direct modulation of a GSL. The method uses two lasers driven with a signal composed of NRZ data and an RF sinusoid. The generated PPM pulses were transmitted over different fiber links by using GS-DFBs and EI GS-DFBs. The obtained results show that the system can provide error-free performance over 10 km with an EI GS-DFB. A degraded performance is also achievable with an uninjected GS-DFB at 10 km. Since these radio systems typically operate with a BER worse than 10^{-3}, this performance may also be acceptable and offers a simpler transmitter design. There is thus a trade-off between the cost/complexity of the transmitter configuration in a UWB-over-fiber system and the required reach and performance of the distribution network. The noise effects caused by pulse propagation from the different sources means that one must choose the transmitter based on the required reach of the network.

TABLE III
COMPARISON BETWEEN THE TWO APPROACH SETUPS IN TERMS OF THEIR LIMITING FACTORS

Approach Setup	Laser Configuration	Costs	Limiting Factors
External modulators	FP-LD	$	• MPN resulting from the energy fluctuations in the longitudinal modes due to dispersive transmission
	DFB-LD	$$$	• SMSR degradation causes MPN problems • Large inherent timing jitter in the generated gain-switching pulses
	EI DFB-LD	$$$$	• Attenuation and dispersion effect
Direct modulation	DFB-LD	$$	• Timing jitter in GS pulses • SMSR degradation causes MPN problems
	EI DFB-LD	$$$	• Degraded extinction ratio

ACKNOWLEDGMENTS

This work was supported in part by the Science Foundation Ireland Research Frontiers Programme and the Enterprise Ireland Technology Development Programme.

REFERENCES

[1] G. R. Allio and G. D. Rogerson, "Ultra-wideband wireless systems," *IEEE Microw. Mag.*, vol. 4, no. 2, pp. 36–47, June 2003.

[2] D. Porcino and W. Hirt, "Ultra-wideband radio technology: potential and challenges ahead," *IEEE Commun. Mag.*, vol. 41, no. 7, pp. 66–74, July 2003.

[3] Federal Communications Commission, "Revision of Part 15 of the Commission's Rules Regarding Ultra-Wideband Transmission Systems," First Note and Order, ET Docket 98-153, FCC 02-8, 2002.

[4] M. Z. Win and R. A. Scholtz, "Ultra-wide bandwidth time-hopping spread spectrum impulse radio for wireless-access communications," *IEEE Trans. Commun.*, vol. 48, no. 4, pp. 679–689, Apr. 2000.

[5] M. Y. Wah, C. Yee, and M. L. Yee, "Wireless ultra wideband communications using radio over fiber," in *IEEE Conf. of Ultra Wideband Systems Technology*, 2006, pp. 265–269.

[6] Y. L. Guennec, M. Lourdiane, B. Cabon, G. Maury, and P. Lombard, "Technologies for UWB-over-fiber," in *IEEE Laser and Electro-Optics Society*, Oct. 2006, pp. 518–519.

[7] W. P. Lin and J. Y. Chen, "Implementation of a new ultrawideband impulse system," *IEEE Photon. Technol. Lett.*, vol. 17, no. 11, pp. 2418–2420, Nov. 2005.

[8] J. Yao, F. Zeng, and Q. Wan, "Photonic generation of ultrawideband signals," *J. Lightwave Technol.*, vol. 25, no. 11, pp. 3219–3235, Nov. 2007.

[9] M. Hanawa, K. Mori, K. Nakamura, A. Matsui, Y. Kanda, and K. Nonaka, "An experimental demonstration of UWB-IR-over-fiber system," in *OFC/NFOEC Conf. on Optical Fiber Communication/Nat. Fiber Optic Engineers Conf.*, 2008, pp. 1–3.

[10] M. Hanawa, K. Mori, K. Nakamura, A. Matsui, Y. Kanda, and K. Nonaka, "Dispersion tolerant UWB-IR-over-fiber transmission under FCC indoor spectrum mask," in *Optical Fiber Communication Conf.*, 2009, paper OTuJ3.

[11] W. Lin, "Biphase impulse generation by a new optical scheme for ultrawide-band radio-over-fiber systems," in *2006 Int. Conf. on Transparent Optical Networks*, 2006, pp. 234.

[12] X. Chen and S. Kiaei, "Monocycle shapes for ultra wideband system," in *Proc. of IEEE Int. Symp. on Circuits and Systems*, 2002, pp. 1597–1600.

[13] R. C. Qiu, H. P. Liu, and X. Shen, "Ultra-wideband for multiple access," *IEEE Commun. Mag.*, vol. 43, no. 2, pp. 80–87, Feb. 2005.

[14] A. Kaszubowska-Anandarajah, P. Perry, L. P. Barry, and H. Shams, "An IR-UWB photonic distribution system," *IEEE Photon. Technol. Lett.*, vol. 20, no. 22, pp. 1884–1886, Nov. 2008.

[15] M. J. L. Cahill, G. J. Pendock, and D. D. Sampson, "Low error rate return-to-zero direct modulation of gain-switched lasers," *Opt. Quantum Electron.*, vol. 28, pp. 1181–1185, 1996.

[16] S. Myong and D. S. Seo, "Pattern independent direct pulse modulation of a gain-switched distributed feedback laser at 2.5 Gbit/s," in *Pacific Rim Conf. on Lasers and Electro-Optics*, vol. 2, 1999, pp. 489–490.

[17] P. M. Anandarajah, C. Guignard, A. Clarke, D. Reid, M. Rensing, L. P. Barry, and J. D. Harvey, "Optimized pulse source employing an externally injected gain-switched laser diode in conjuction with a nonlinearly chirped grating," *IEEE J. Sel. Top. Quantum Electron.*, vol. 12, no. 2, pp. 255–264, Mar.–Apr. 2006.

[18] L. P. Barry and P. Anandarajah, "Effect of side-mode suppression ratio on the performance of self-seeded gain-switched optical pulses in lightwave communications systems," *IEEE Photon. Technol. Lett.*, vol. 11, no. 11, pp. 1360–1362, Nov. 1999.

[19] A. Clarke, P. Anandarajah, and L. P. Barry, "Generation of widely tunable picosecond pulses with large SMSR by externally injecting a gain-switched dual laser source," *IEEE Photon. Technol. Lett.*, vol. 16, no. 10, pp. 2344–2346, Oct. 2006.

[20] C. Lin and J. K. Andersen, "Frequency chirp reduction in a 2.2 Gbit/s directly modulated InGaAsP semiconductor laser by CW injection," *Electron. Lett.*, vol. 21, no. 2, pp. 80–81, 1985.